World Journal of Mechanics, 2012, 2, 297-310
doi:10.4236/wjm.2012.26036 Published Online December 2012 (http://www.SciRP.org/journal/wjm)

Free Vibration Analysis of Functionally Graded Beams with General Elastically End Constraints by DTM

Nuttawit Wattanasakulpong[1*], Variddhi Ungbhakorn[2]
[1]Department of Mechanical Engineering, Mahanakorn University of Technology, Bangkok, Thailand
[2]Department of Mechanical Engineering, Chulalongkorn University, Bangkok, Thailand
Email: *nuttawit_mut@hotmail.com, v_ungbhakorn@yahoo.com

Received August 24, 2012; revised September 25, 2012; accepted October 10, 2012

ABSTRACT

The differential transformation method (DTM) is applied to investigate free vibration of functionally graded beams supported by arbitrary boundary conditions, including various types of elastically end constraints. The material properties of functionally graded beams are assumed to obey the power law distribution. The main advantages of this method are known for its excellence in high accuracy with small computational expensiveness. The DTM also provides all natural frequencies and mode shapes without any frequency missing. Fundamental frequencies as well as their higher frequencies and mode shapes are presented. The significant aspects such as boundary conditions, values of translational and rotational spring constants and the material volume fraction index on the natural frequencies and mode shapes are discussed. For elastically end constraints, some available results of special cases for isotropic beams are used to validate the present results. The new frequency results and mode shapes of functionally graded beams resting on elastically end constraints are presented.

Keywords: Functionally Graded Beams; Free Vibration; Natural Frequency; Mode Shape; Differential Transformation Method

1. Introduction

A new class of composite materials, called functionally graded materials (FGMs), is considered in this paper. The potential uses of FGMs in engineering applications include aerospace structures, engine combustion chambers, fusion energy devices, engine parts and other engineering structures. In recent years, the static and dynamic analyses of functionally graded (FG) beams have increasingly attracted many researchers.

Sankar [1] provided an elasticity solution based on Euler-Bernoulli beam theory for bending analysis of FG beams. An analytical solution of cantilever FG beams subjected to various types of loadings was presented by Zhong and Yu [2] using the Airy stress function. Deflection and natural frequency results of the layered FG beams were obtained from the zigzag theoretical modeling and experiment by Kapuria *et al*. [3]. Sina *et al*. [4] employed the first order shear deformation (FSDT) to solve the free vibration problem of FG beams. The Lagrange multiplier method was used to solve the fundamental frequency of FG beams based on different higher-order beam theories in the study of Simsek [5]. Free vibration analysis of simply supported FG beams was done by Aydogdu and Taskin [6]. Wattanasakulpong *et al*. [7] used an improved third order shear deformation theory to analyze free vibration of FG beams using the Ritz method. The finite element method was used by Alshorbagy *et al*. [8] to investigate free vibration characteristics of FG beams. Yang and Chen [9] provided analytical solution based on classical beam theory (CBT) for investigating natural frequencies and critical buckling load of FG beams with edge cracks. The edge cracked FG beams were also studied by Kitipornchai *et al*. [10] using Timoshenko beam theory. The problems of FG beams resting on elastic foundations were solved by Sahraee *et al*. [11] and Pradhan and Murmu [12] using differential quadrature method (DQM). Isotropic beams, supported by elastically end constraints, were the subject of many researchers [13-16], but none is dealing with FG beams.

Differential transformation method (DTM) based on Taylor series expansion was initially introduced by Zhou [17] in his study of electrical circuits. It was first implemented to solve vibration analysis of beams by Malik and Dang [18]. Kaya and Ozgumus [19-21] successfully used the DTM to solve many cases of vibration problems. Pradhan *et al*. [22] also used the DTM to solve the buckling problem of a single walled carbon nanotube.

According to the authors' knowledge, there is no pre-

*Corresponding author.

vious study on free vibration of FG beams supported by elastically end constraints in the open literature. In this study, the effective tool, DTM, is implemented to analyze free vibration of FG beams with arbitrary boundary conditions, including various types of elastically end constraints. Fundamental frequencies as well as their higher frequencies and mode shapes are presented. The effects of spring constants and the material volume fraction index on the natural frequencies and mode shapes are discussed. Some available special cases in the open literature are used to validate the present results derived from DTM.

2. Functionally Graded Materials

A functionally graded beam made of ceramic-metal is considered in this study. The beam geometry and the variation of material volume fraction across the beam thickness associated with the power law distribution are shown in **Figure 1**.

Based on the rule of mixture, the effective material properties, P, can be written as

$$P = P_m V_m + P_c V_c \tag{1}$$

where P_m, P_c, V_m and V_c are material properties and the volume fraction of the metal and ceramic respectively with the relation

$$V_m + V_c = 1. \tag{2}$$

According to the power law distribution, the volume fraction of ceramic can be written as

$$V_c = \left(\frac{z}{h} + \frac{1}{2}\right)^n \tag{3}$$

where the positive number, $0 \le n \le \infty$, is the power law or volume fraction index. The FG beam becomes a fully ceramic beam when n is set to zero. From the above relationship, the material properties, in terms of Young's modulus and mass density are expressed as

$$E(z) = (E_c - E_m)\left(\frac{z}{h} + \frac{1}{2}\right)^n + E_m, \tag{4a}$$

$$\rho(z) = (\rho_c - \rho_m)\left(\frac{z}{h} + \frac{1}{2}\right)^n + \rho_m. \tag{4b}$$

Delale and Erdogan [23] indicated that the effect of Poisson's ratio on the behavior of the FG plate is much less than that of the Young's modulus, thus the Poisson's ratio will assume to be constant in our study.

3. The FGM Beam Vibration Analysis

Consider a classical beam theory (CBT) based on the Kirchhoff-Love hypothesis, the displacements of an arbitrary point along x and z axes can be expressed as follows:

$$u(x,z,t) = u_0 - z\frac{\partial w}{\partial x},\ w(x,z,t) = w_0(x,t). \tag{5}$$

where u_0 and w_0 are the displacements at a point in the mid-plane. From the displacements in Equation (5), one can obtain the non-zero strains of the beam as

$$\varepsilon_{xx} = \frac{\partial u_0}{\partial x} - z\frac{\partial^2 w}{\partial x^2} = \varepsilon_0 - z\xi_x;\ \varepsilon_0 = \frac{\partial u_0}{\partial x}, \xi_x = \frac{\partial^2 w}{\partial x^2}. \tag{6}$$

The normal force resultant, N_x, moment resultant, M_x, and transverse shear force, Q_x, take the form:

$$N_x = A_{11}\varepsilon_0 - B_{11}\xi_x, \tag{7a}$$

$$M_x = B_{11}\varepsilon_0 - D_{11}\xi_x, \tag{7b}$$

$$Q_x = \frac{\partial M_x}{\partial x} = B_{11}\frac{\partial \varepsilon_0}{\partial x} - D_{11}\frac{\partial \xi_x}{\partial x}, \tag{7c}$$

where

$$(A_{11}, B_{11}, D_{11}) = \int_{-h/2}^{h/2} \frac{E(z)}{\left[1-\nu^2\right]}(1, z, z^2)\,\mathrm{d}z. \tag{8}$$

The extensional stiffness (A_{11}), extensional-bending

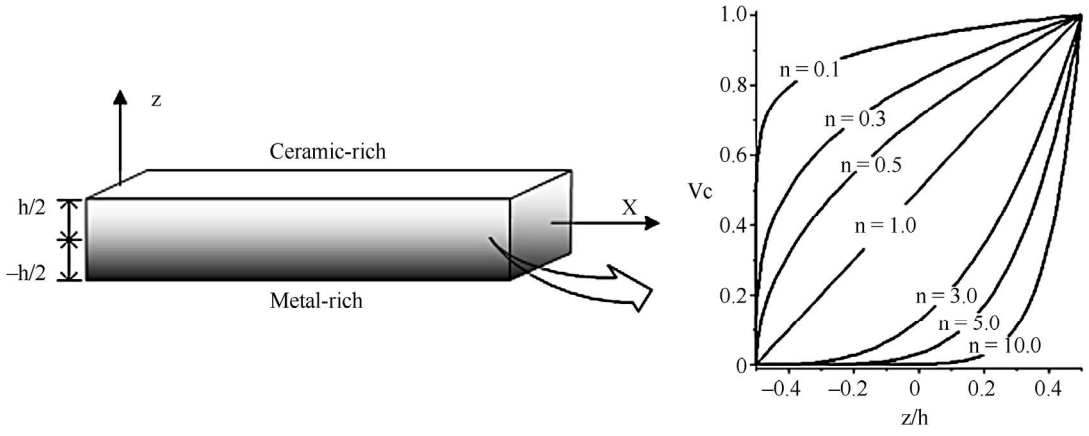

Figure 1. Geometry of a functionally graded beam and volume fraction profile.

coupling stiffness (B_{11}) and bending stiffness (D_{11}) can be written in the function of the volume faction index (n) as:

$$A_{11} = \frac{h}{1-\nu^2}\left[\frac{(E_c - E_m)}{(n+1)} + E_m\right] \tag{9a}$$

$$B_{11} = \frac{(E_c - E_m)h^2}{1-\nu^2}\left[\frac{n}{2(n+1)(n+2)}\right] \tag{9b}$$

$$D_{11} = \frac{h^3}{1-\nu^2}\left[\frac{(E_c - E_m)(n^2+n+2)}{4(n+1)(n+2)(n+3)} + \frac{E_m}{12}\right] \tag{9c}$$

The axial inertia term is neglected, therefore, the governing equations of the FG beams derived from Hamilton's principle can be expressed as follows:

$$\delta u_0 : \frac{\partial N_x}{\partial x} = 0 \rightarrow A_{11}\frac{\partial^2 u_0}{\partial x^2} - B_{11}\frac{\partial^3 w}{\partial x^3} = 0, \tag{10}$$

$$\delta w : \frac{-\partial^2 M_x}{\partial x} + I_0\frac{\partial^2 w}{\partial t^2} = 0 \rightarrow \left(D_{11} - \frac{B_{11}^2}{A_{11}}\right)\frac{\partial^4 w}{\partial x^4} + I_0\frac{\partial^2 w}{\partial t^2} = 0. \tag{11}$$

Substituting harmonic vibration mode, $w = We^{i\omega t}$, into Equation (11) leads to a time independent governing equation as follows:

$$\left(D_{11} - \frac{B_{11}^2}{A_{11}}\right)\frac{\partial^4 W}{\partial x^4} - I_0\omega^2 W = 0. \tag{12}$$

where ω is a natural frequency and $I_0 = \int_{-h/2}^{h/2}\rho(z)\mathrm{d}z$ is the moment of inertia which can be expressed in term of the volume faction index as:

$$I_0 = h\left[\frac{(\rho_c - \rho_m)}{(n+1)} + \rho_m\right]. \tag{13}$$

4. Application of DTM to FG Beam Vibration Analysis

The principle of the DTM is to transform the governing differential and boundary condition equations into a set of algebraic equations using transformation rules. The basic operations required in differential transformation for the governing differential and boundary condition equations are shown in **Tables 1** and **2** respectively.

The general function, $f(x)$ in **Tables 1** and **2** is considered as the transverse displacement $W(x)$. Apply the basic operations of DTM in **Table 1** with the fundamentals of the DTM presented in [18] to the governing differential equation, Equation (12), one can obtain the recurrence equation as:

$$W[r+4] = \frac{I_0\omega^2}{\lambda(r+1)(r+2)(r+3)(r+4)}W[r] \tag{14}$$

where $\lambda = \left(D_{11} - \frac{B_{11}^2}{A_{11}}\right)$.

It is seen that Equation (14) is independent from boundary conditions. Therefore to obtain frequency results, the displacement function of Equation (14) must be used to satisfy the corresponding boundary equations.

4.1. FG beams without Elastically End Constraints

Three types of general edge conditions, without any springs, at x = 0 and L are: Simply supported (S),

Table 1. Basic operations of DTM for the governing equations.

Original functions	*Transformed functions*
$f(x) = g(x) \pm h(x)$	$F[r] = G[r] \pm H[r]$
$f(x) = \lambda g(x)$	$F[r] = \lambda G[r]$
$f(x) = g(x)h(x)$	$F[r] = \sum_{l=0}^{r} G[r-l]H[l]$
$f(x) = \frac{\mathrm{d}^p g(x)}{\mathrm{d}x^p}$	$F[r] = \frac{(r+p)!}{r!}G[r+p]$
$f(x) = x^p$	$F[r] = \delta(r-p) = \begin{cases} 0 & r \neq p \\ 1 & r = p \end{cases}$

Table 2. Basic operations of DTM for the boundary conditions.

$x = 0$		$x = L$	
Original B.C.	*Transformed B.C.*	*Original B.C.*	*Transformed B.C.*
$f(0) = 0$	$F(0) = 0$	$f(L) = 0$	$\sum_{r=0}^{\infty} L^{(r)}F(r) = 0$
$\frac{\mathrm{d}f(0)}{\mathrm{d}x} = 0$	$F(1) = 0$	$\frac{\mathrm{d}f(L)}{\mathrm{d}x} = 0$	$\sum_{r=0}^{\infty} rL^{(r-1)}F(r) = 0$
$\frac{\mathrm{d}^2 f(0)}{\mathrm{d}x^2} = 0$	$F(2) = 0$	$\frac{\mathrm{d}^2 f(L)}{\mathrm{d}x^2} = 0$	$\sum_{r=0}^{\infty} r(r-1)L^{(r-2)}F(r) = 0$
$\frac{\mathrm{d}^3 f(0)}{\mathrm{d}x^3} = 0$	$F(3) = 0$	$\frac{\mathrm{d}^3 f(L)}{\mathrm{d}x^3} = 0$	$\sum_{r=0}^{\infty} r(r-1)(r-2)L^{(r-3)}F(r) = 0$

$W = 0$, $\dfrac{\mathrm{d}^2W}{\mathrm{d}x^2} = 0$; Clamped (C), $W = 0$, $\dfrac{\mathrm{d}W}{\mathrm{d}x} = 0$; and Free (F), $\dfrac{\mathrm{d}^2W}{\mathrm{d}x^2} = 0$, $\dfrac{\mathrm{d}^3W}{\mathrm{d}x^3} = 0$. Now consider a beam with free-free (F-F) boundary conditions. The bending moment and shear force at $x = 0$ and L are zero. Let the non-zero values of deflection and slope at $x = 0$ indicate by C_0 and C_1 respectively. Applying the basic operations of DTM for the boundary condition at $x = 0$, using **Table 2**, one obtains

$$W[0] = C_0, W[1] = C_1, W[2] = 0, W[3] = 0. \tag{15}$$

Substituting Equation (15) into the recurrence equation Equation (14) leads to $W[r]$ for all values of r as follows:

$$W[4r] = \frac{\omega^{2r} I_0^r}{\lambda^r (4r)!} C_0 \qquad r = 0,1,2,3,\cdots \tag{16a}$$

$$W[4r+1] = \frac{\omega^{2r} I_0^r}{\lambda^r (4r+1)!} C_1 \qquad r = 0,1,2,3,\cdots \tag{16b}$$

$$W[4r+2] = 0 \qquad r = 0,1,2,3,\cdots \tag{16c}$$

$$W[4r+3] = 0 \qquad r = 0,1,2,3,\cdots \tag{16d}$$

For the boundary condition at $x = L$, applying the basic operations of DTM using **Table 2**, one obtains

$$\begin{aligned} &\sum_{r=0}^{\infty} r(r-1) L^{(r-2)} W[r] = 0, \\ &\sum_{r=0}^{\infty} r(r-1)(r-2) L^{(r-3)} W[r] = 0 \end{aligned} \tag{17}$$

Substituting $W[r]$ from Equation (16) into Equation (17) leads to two polynomial equations which can be arranged into the following matrix form.

$$\begin{bmatrix} e_{11} & e_{12} \\ e_{21} & e_{22} \end{bmatrix} \begin{Bmatrix} C_0 \\ C_1 \end{Bmatrix} = \begin{Bmatrix} 0 \\ 0 \end{Bmatrix} \tag{18}$$

where

$$e_{11} = \sum_{r=1}^{\infty} \frac{\omega^{2r} I_0^r L^{(4r-2)}}{\lambda^r (4r-2)!}; \quad e_{12} = \sum_{r=1}^{\infty} \frac{\omega^{2r} I_0^r L^{(4r-1)}}{\lambda^r (4r-1)!};$$

$$e_{21} = \sum_{r=1}^{\infty} \frac{\omega^{2r} I_0^r L^{(4r-3)}}{\lambda^r (4r-3)!}; \quad e_{22} = \sum_{r=1}^{\infty} \frac{\omega^{2r} I_0^r L^{(4r-2)}}{\lambda^r (4r-2)!}.$$

The frequency results can be determined by setting the determinant of the coefficient matrix of Equation (18) to zero. Hence, the frequency equation can be expressed with the finite number of terms in each component of the matrix from r to R as:

$$\begin{aligned} &\sum_{r=1}^{R} \frac{\omega^{2r} I_0^r L^{(4r-2)}}{\lambda^r (4r-2)!} \times \sum_{r=1}^{R} \frac{\omega^{2r} I_0^r L^{(4r-2)}}{\lambda^r (4r-2)!} \\ &- \sum_{r=1}^{R} \frac{\omega^{2r} I_0^r L^{(4r-3)}}{\lambda^r (4r-3)!} \times \sum_{r=1}^{R} \frac{\omega^{2r} I_0^r L^{(4r-1)}}{\lambda^r (4r-1)!} = 0 \end{aligned} \tag{19}$$

Solving the frequency equation in Equation (19), one obtains the frequency results as: $\omega = \omega_r^{[R]}$, where $r = 1, 2, 3, \cdots, R$. Therefore, $\omega_r^{[R]}$ is the r^{th} estimated frequency corresponding to R. Hence, an appropriate value of R is obtained by convergence analysis with the following criterion,

$$\left| \omega_r^{[R]} - \omega_r^{[R-1]} \right| \le \delta \tag{20}$$

where δ is a given error tolerance.

The mode shape function can be obtained using $W(x) = \sum_{r=0}^{R} x^r W[r]$, that is

$$\begin{aligned} W(x) = &\sum_{r=0}^{R} \frac{\omega^{2r} I_0^r}{\lambda^r (4r)!} x^{(4r)} \\ &- \frac{\sum_{r=1}^{R} \dfrac{\omega^{2r} I_0^r L^{(4r-2)}}{\lambda^r (4r-2)!}}{\sum_{r=1}^{R} \dfrac{\omega^{2r} I_0^r L^{(4r-1)}}{\lambda^r (4r-1)!}} \sum_{r=0}^{R} \frac{\omega^{2r} I_0^r}{\lambda^r (4r+1)!} x^{(4r+1)} \end{aligned} \tag{21}$$

Following the same procedure, one can obtain the frequency equation and mode shape function for other kinds of boundary conditions without any spring support as given in Appendix A.

4.2. FG Beams with Elastically End Constraints

A FG beam supporting by elastic translational and rotational springs at both ends, called E-E boundary conditions, is shown in **Figure 2**. For this case, the boundary conditions at the left end can be expressed as,

$$k_{TL} W + Q_x = 0, \quad k_{RL} \frac{\mathrm{d}W}{\mathrm{d}x} - M_x = 0. \tag{22}$$

The boundary conditions in Equation (22) can be take another form as

$$\frac{\mathrm{d}^3W}{\mathrm{d}x^3} + \frac{k_{TL}}{\lambda} W = 0, \quad \frac{\mathrm{d}^2W}{\mathrm{d}x^2} - \frac{k_{RL}}{\lambda} \frac{\mathrm{d}W}{\mathrm{d}x} = 0. \tag{23}$$

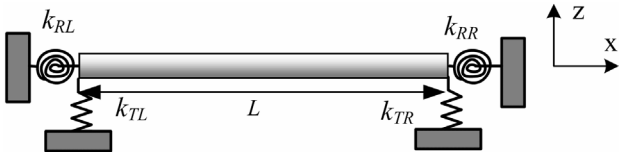

Figure 2. Geometry of FG beam with E-E boundary condition.

Where k_{TL} and k_{RL} are the translational spring constant (MN/m) and the rotational spring constant (MN·m/rad) at the left end respectively. Let the non-zero values of deflection and slope at $x = 0$ be C_0 and C_1 respectively. Use **Table 2** to apply the basic operations of DTM for these non-zero quantities at $x = 0$, one obtains

$$W[0] = W(x) = C_0, \quad W[1] = \frac{\mathrm{d}W(x)}{\mathrm{d}x} = C_1. \tag{24}$$

The expressions for non-zero values of bending moment and shear force at $x = 0$ can be written as

$$W[2] = \frac{k_{RL}C_1}{2\lambda}, \quad W[3] = -\frac{k_{TL}C_0}{6\lambda}. \tag{25}$$

To find $W[r]$ for all values of r, the components in Equations (24) and (25) are substituted into the recurrence Equation (14).

$$W[4r] = \frac{\omega^{2r} I_0^r C_0}{\lambda^r (4r)!}, \quad r = 0,1,2,3,\cdots. \tag{26a}$$

$$W[4r] = \frac{\omega^{2r} I_0^r C_0}{\lambda^r (4r)!}, \quad r = 0,1,2,3,\cdots. \tag{26b}$$

$$W[4r+2] = \frac{\omega^{2r} I_0^r k_{RL} C_1}{\lambda^{(r+1)} (4r+2)!}, \quad r = 0,1,2,3,\cdots. \tag{26c}$$

$$W[4r+3] = -\frac{\omega^{2r} I_0^r k_{TL} C_0}{\lambda^{(r+1)} (4r+3)!}, \quad r = 0,1,2,3,\cdots. \tag{26d}$$

At $x = L$, the boundary conditions are

$$k_{RR}\frac{\mathrm{d}W}{\mathrm{d}x} + M_x = 0, \quad k_{TR}W - Q_x = 0. \tag{27}$$

They can be written as:

$$\frac{\mathrm{d}^2 W}{\mathrm{d}x^2} + \frac{k_{RR}}{\lambda}\frac{\mathrm{d}W}{\mathrm{d}x} = 0, \quad \frac{\mathrm{d}^3 W}{\mathrm{d}x^3} - \frac{k_{TR}}{\lambda}W = 0. \tag{28}$$

Similarly, applying the DTM to the boundary conditions (28) yields

$$\sum_{r=0}^{\infty} r(r-1)L^{(r-2)}W[r] + \frac{k_{RR}}{\lambda}\sum_{r=0}^{\infty} rL^{(r-1)}W[r] = 0, \tag{29a}$$

$$\sum_{r=0}^{\infty} r(r-1)(r-2)L^{(r-3)}W[r] - \frac{k_{TR}}{\lambda}\sum_{r=0}^{\infty} L^{(r)}W[r] = 0. \tag{29b}$$

Substituting $W[r]$ from Equation (26) into Equation (29) leads to two polynomial equations which can be arranged into the following matrix form:

$$\begin{bmatrix} p_{11} & p_{12} \\ p_{21} & p_{22} \end{bmatrix} \begin{Bmatrix} C_0 \\ C_1 \end{Bmatrix} = \begin{Bmatrix} 0 \\ 0 \end{Bmatrix} \tag{30}$$

where:

$$p_{11} = \sum_{r=1}^{\infty} \frac{L^{(4r-2)}\omega^{2r} I_0^r}{\lambda^r (4r-2)!} + k_{RR}\sum_{r=1}^{\infty} \frac{L^{(4r-1)}\omega^{2r} I_0^r}{\lambda^{(r+1)} (4r-1)!} - k_{TL}\sum_{r=0}^{\infty} \frac{L^{(4r+1)}\omega^{2r} I_0^r}{\lambda^{(r+1)} (4r+1)!} - k_{RR}k_{TL}\sum_{r=0}^{\infty} \frac{L^{(4r+2)}\omega^{2r} I_0^r}{\lambda^{(r+2)} (4r+2)!}$$

$$p_{12} = \sum_{r=1}^{\infty} \frac{L^{(4r-1)}\omega^{2r} I_0^r}{\lambda^r (4r-1)!} + k_{RR}\sum_{r=0}^{\infty} \frac{L^{(4r)}\omega^{2r} I_0^r}{\lambda^{(r+1)} (4r)!} + k_{RL}\sum_{r=0}^{\infty} \frac{L^{(4r)}\omega^{2r} I_0^r}{\lambda^{(r+1)} (4r)!} + k_{RR}k_{RL}\sum_{r=0}^{\infty} \frac{L^{(4r+1)}\omega^{2r} I_0^r}{\lambda^{(r+2)} (4r+1)!}$$

$$p_{21} = \sum_{r=1}^{\infty} \frac{L^{(4r-3)}\omega^{2r} I_0^r}{\lambda^r (4r-3)!} - k_{TR}\sum_{r=0}^{\infty} \frac{L^{(4r)}\omega^{2r} I_0^r}{\lambda^{(r+1)} (4r)!} - k_{TL}\sum_{r=0}^{\infty} \frac{L^{(4r)}\omega^{2r} I_0^r}{\lambda^{(r+1)} (4r)!} + k_{TR}k_{TL}\sum_{r=0}^{\infty} \frac{L^{(4r+3)}\omega^{2r} I_0^r}{\lambda^{(r+2)} (4r+3)!}$$

$$p_{22} = \sum_{r=1}^{\infty} \frac{L^{(4r-2)}\omega^{2r} I_0^r}{\lambda^r (4r-2)!} - k_{TR}\sum_{r=0}^{\infty} \frac{L^{(4r+1)}\omega^{2r} I_0^r}{\lambda^{(r+1)} (4r+1)!} + k_{RL}\sum_{r=1}^{\infty} \frac{L^{(4r-1)}\omega^{2r} I_0^r}{\lambda^{(r+1)} (4r-1)!} - k_{TR}k_{RL}\sum_{r=0}^{\infty} \frac{L^{(4r+2)}\omega^{2r} I_0^r}{\lambda^{(r+2)} (4r+2)!}.$$

Similarly, set the determinant of the coefficient matrix of Equation (30) to zero with finite number of terms, one obtains the following frequency equation.

$$\begin{aligned}
&\left[\sum_{r=1}^{R}\left(\frac{L^{(4r-2)}\omega^{2r} I_0^r}{\lambda^r (4r-2)!} + k_{RR}\frac{L^{(4r-1)}\omega^{2r} I_0^r}{\lambda^{(r+1)} (4r-1)!}\right) - \sum_{r=0}^{R}\left(k_{TL}\frac{L^{(4r+1)}\omega^{2r} I_0^r}{\lambda^{(r+1)} (4r+1)!} + k_{RR}k_{TL}\frac{L^{(4r+2)}\omega^{2r} I_0^r}{\lambda^{(r+2)} (4r+2)!}\right)\right] \\
&\times\left[\sum_{r=1}^{R}\left(\frac{L^{(4r-2)}\omega^{2r} I_0^r}{\lambda^r (4r-2)!} + k_{RL}\frac{L^{(4r-1)}\omega^{2r} I_0^r}{\lambda^{(r+1)} (4r-1)!}\right) - \sum_{r=0}^{R}\left(k_{TR}\frac{L^{(4r+1)}\omega^{2r} I_0^r}{\lambda^{(r+1)} (4r+1)!} + k_{TR}k_{RL}\frac{L^{(4r+2)}\omega^{2r} I_0^r}{\lambda^{(r+2)} (4r+2)!}\right)\right] \\
&-\left[\sum_{r=1}^{R}\frac{L^{(4r-3)}\omega^{2r} I_0^r}{\lambda^r (4r-3)!} + \sum_{r=0}^{R}\left(k_{TR}k_{TL}\frac{L^{(4r+3)}\omega^{2r} I_0^r}{\lambda^{(r+2)} (4r+3)!} - k_{TR}\frac{L^{(4r)}\omega^{2r} I_0^r}{\lambda^{(r+1)} (4r)!} - k_{TL}\frac{L^{(4r)}\omega^{2r} I_0^r}{\lambda^{(r+1)} (4r)!}\right)\right] \\
&\times\left[\sum_{r=1}^{R}\frac{L^{(4r-1)}\omega^{2r} I_0^r}{\lambda^r (4r-1)!} + \sum_{r=0}^{R}\left(k_{RR}k_{RL}\frac{L^{(4r+1)}\omega^{2r} I_0^r}{\lambda^{(r+2)} (4r+1)!} + k_{RR}\frac{L^{(4r)}\omega^{2r} I_0^r}{\lambda^{(r+1)} (4r)!} + k_{RL}\frac{L^{(4r)}\omega^{2r} I_0^r}{\lambda^{(r+1)} (4r)!}\right)\right] = 0
\end{aligned} \tag{31}$$

The mode shape function corresponding to the frequency in Equation (31) can be derived as:

$$W(x) = \left[\sum_{r=0}^{R}\frac{\omega^{2r}I_0^r}{\lambda^r(4r)!}x^{(4r)} + C_1\sum_{r=0}^{R}\frac{\omega^{2r}I_0^r}{\lambda^r(4r+1)!}x^{(4r+1)} + C_1\sum_{r=0}^{R}\frac{\omega^{2r}I_0^r k_{RL}}{\lambda^{(r+1)}(4r+2)!}x^{(4r+2)} - \sum_{r=0}^{R}\frac{\omega^{2r}I_0^r k_{TL}}{\lambda^{(r+1)}(4r+3)!}x^{(4r+3)}\right] \tag{32}$$

where: (please see the Equation (33) below).

Following similar procedure, one can obtain the frequency equation and mode shape function for a clamped-elastic supported (C-E) beam in **Figure 3** as follows.

The frequency equation:

$$\begin{aligned}&\left[\sum_{r=0}^{R}\left(\frac{L^{(4r)}\omega^{2r}I_0^r}{\lambda^r(4r)!} + k_{RR}\frac{L^{(4r+1)}\omega^{2r}I_0^r}{\lambda^{(r+1)}(4r+1)!}\right)\right]\\ &\times\left[\sum_{r=0}^{R}\left(\frac{L^{(4r)}\omega^{2r}I_0^r}{\lambda^r(4r)!} - k_{TR}\frac{L^{(4r+3)}\omega^{2r}I_0^r}{\lambda^{(r+1)}(4r+3)!}\right)\right]\\ &-\left[\sum_{r=1}^{R}\frac{L^{(4r-1)}\omega^{2r}I_0^r}{\lambda^r(4r-1)!} - k_{TR}\sum_{r=0}^{R}\frac{L^{(4r+2)}\omega^{2r}I_0^r}{\lambda^{(r+1)}(4r+2)!}\right]\\ &\times\left[\sum_{r=0}^{R}\left(\frac{L^{(4r+1)}\omega^{2r}I_0^r}{\lambda^r(4r+1)!} + k_{RR}\frac{L^{(4r+2)}\omega^{2r}I_0^r}{\lambda^{(r+1)}(4r+2)!}\right)\right] = 0\end{aligned} \tag{34}$$

The mode shape function:

$$W(x) = \sum_{r=0}^{R}\frac{\omega^{2r}I_0^r}{\lambda^r(4r+2)!}x^{(4r+2)} + C_1\sum_{r=0}^{R}\frac{\omega^{2r}I_0^r}{\lambda^r(4r+3)!}x^{(4r+3)} \tag{35}$$

where:

$$C_1 = -\frac{\sum_{r=0}^{R}\left(\frac{L^{(4r)}\omega^{2r}I_0^r}{\lambda^r(4r)!} + k_{RR}\frac{L^{(4r+1)}\omega^{2r}I_0^r}{\lambda^{(r+1)}(4r+1)!}\right)}{\sum_{r=0}^{R}\left(\frac{L^{(4r+1)}\omega^{2r}I_0^r}{\lambda^r(4r+1)!} + k_{RR}\frac{L^{(4r+2)}\omega^{2r}I_0^r}{\lambda^{(r+1)}(4r+2)!}\right)}. \tag{36}$$

For the case of simply supported-elastic (S-E) FG beams as shown in **Figure 4**, the expressions for the frequency equation and the mode shape function can be written as:

The frequency equation:

$$\begin{aligned}&\left[\sum_{r=1}^{R}\frac{L^{(4r-1)}\omega^{2r}I_0^r}{\lambda^r(4r-1)!} + k_{RR}\sum_{r=0}^{R}\frac{L^{(4r)}\omega^{2r}I_0^r}{\lambda^{(r+1)}(4r)!}\right]\\ &\times\left[\sum_{r=0}^{R}\left(\frac{L^{(4r)}\omega^{2r}I_0^r}{\lambda^r(4r)!} - k_{TR}\frac{L^{(4r+3)}\omega^{2r}I_0^r}{\lambda^{(r+1)}(4r+3)!}\right)\right]\\ &-\left[\sum_{r=1}^{R}\frac{L^{(4r-2)}\omega^{2r}I_0^r}{\lambda^r(4r-2)!} - k_{TR}\sum_{r=0}^{R}\frac{L^{(4r+1)}\omega^{2r}I_0^r}{\lambda^{(r+1)}(4r+1)!}\right]\\ &\times\left[\sum_{r=0}^{R}\left(\frac{L^{(4r+1)}\omega^{2r}I_0^r}{\lambda^r(4r+1)!} + k_{RR}\frac{L^{(4r+2)}\omega^{2r}I_0^r}{\lambda^{(r+1)}(4r+2)!}\right)\right] = 0\end{aligned} \tag{37}$$

The mode shape function:

$$W(x) = \sum_{r=0}^{R}\frac{\omega^{2r}I_0^r}{\lambda^r(4r+1)!}x^{(4r+1)} + C_1\sum_{r=0}^{R}\frac{\omega^{2r}I_0^r}{\lambda^r(4r+3)!}x^{(4r+3)} \tag{38}$$

where

$$C_1 = -\frac{\sum_{r=1}^{R}\frac{L^{(4r-1)}\omega^{2r}I_0^r}{\lambda^r(4r-1)!} + k_{RR}\sum_{r=0}^{R}\frac{L^{(4r)}\omega^{2r}I_0^r}{\lambda^{(r+1)}(4r)!}}{\sum_{r=0}^{R}\left(\frac{L^{(4r+1)}\omega^{2r}I_0^r}{\lambda^r(4r+1)!} + k_{RR}\frac{L^{(4r+2)}\omega^{2r}I_0^r}{\lambda^{(r+1)}(4r+2)!}\right)} \tag{39}$$

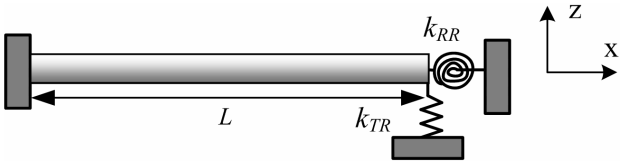

Figure 3. Geometry of FG beam with C-E boundary condition.

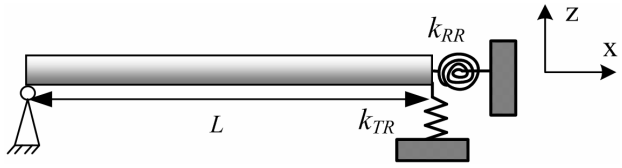

Figure 4. Geometry of FG beam with S-E boundary condition.

$$C_1 = -\frac{\sum_{r=1}^{R}\left(\frac{L^{(4r-2)}\omega^{2r}I_0^r}{\lambda^r(4r-2)!} + k_{RR}\frac{L^{(4r-1)}\omega^{2r}I_0^r}{\lambda^{(r+1)}(4r-1)!}\right) - \sum_{r=0}^{R}\left(k_{TL}\frac{L^{(4r+1)}\omega^{2r}I_0^r}{\lambda^{(r+1)}(4r+1)!} + k_{RR}k_{TL}\frac{L^{(4r+2)}\omega^{2r}I_0^r}{\lambda^{(r+2)}(4r+2)!}\right)}{\sum_{r=1}^{R}\frac{L^{(4r-1)}\omega^{2r}I_0^r}{\lambda^r(4r-1)!} + \sum_{r=0}^{R}\left(k_{RR}k_{RL}\frac{L^{(4r+1)}\omega^{2r}I_0^r}{\lambda^{(r+2)}(4r+1)!} + k_{RR}\frac{L^{(4r)}\omega^{2r}I_0^r}{\lambda^{(r+1)}(4r)!} + k_{RL}\frac{L^{(4r)}\omega^{2r}I_0^r}{\lambda^{(r+1)}(4r)!}\right)}. \tag{33}$$

5. Numerical Results and Discussions

5.1. FG Beams without Elastically End Constraints

FG beams made of Alumina (Al_2O_3) and Aluminum (Al); whose material properties are: E = 380 GPa, ρ = 3960 kg/m^3, ν = 0.3 for Al_2O_3 and E = 70 GPa, ρ = 2702 kg/m^3, ν = 0.3 for Al; are chosen for this study. Six types of boundary conditions are considered as shown in **Table 3**. The dimensionless frequency is defined as $\Omega = \omega L^2 / h\sqrt{(\rho_{Al}/E_{Al})}$. From convergence study it is found out that R equals to 15 is sufficient for the required accuracy. Using R more than 15 will present the same results for the first to sixth modes. To receive the frequency results that are higher than sixth mode, the value of R more than 15 may be needed. Five modes of vibration with various volume fraction indexes are presented in **Table 3**.

Only the fundamental frequencies of the work by Simsek [5] for three types of boundary conditions, namely, (S-S), (C-F) and (C-C), are found in the open literature. Very good agreement with the present results for all volume fraction indexes is confirmed as shown in **Table 3**. It is seen that, for all boundary conditions, all frequencies decrease as volume fraction indexes increase. The C-C and F-F frequencies are practically equal and they are the highest of all boundary conditions. Results in the table show that the volume fraction index is one of the most important parameters that have significant impact on the frequency of vibration and therefore, it must be

Table 3. Dimensionless frequencies of Al_2O_3/Al beams without springs (L/h = 20).

B.C.	Mode	Al_2O_3	n = 0.2	n = 0.5	n = 1.0	n = 2.0	n = 5.0	Al
	Ω_1	5.483 5.478*	5.102 5.098*	4.669 4.665*	4.221 4.216*	3.852 3.847*	3.668 3.663*	2.849 2.846*
	Ω_2	21.933	20.408	18.676	16.884	15.407	14.670	11.396
S-S	Ω_3	49.350	45.917	42.021	37.989	34.667	33.007	25.642
	Ω_4	87.734	81.631	74.703	67.536	61.629	58.680	45.586
	Ω_5	137.082	127.551	116.726	105.528	96.299	91.687	71.227
	Ω_1	1.953 1.952*	1.816 1.817*	1.663 1.663*	1.504 1.503*	1.372 1.371*	1.307 1.306*	1.015 1.015*
	Ω_2	12.242	11.390	10.424	9.424	8.599	8.188	6.361
C-F	Ω_3	34.278	31.893	29.187	26.386	24.079	22.926	17.810
	Ω_4	67.171	62.498	57.194	51.707	47.185	44.926	34.901
	Ω_5	111.037	103.313	94.547	85.474	77.998	74.267	57.694
	Ω_1	12.430 12.414*	11.566 11.554*	10.584 10.571*	9.569 9.555*	8.732 8.719*	8.314 8.301*	6.459 6.450*
	Ω_2	34.264	31.881	29.175	26.376	24.069	22.917	17.803
C-C	Ω_3	67.172	62.499	57.195	51.707	47.185	44.927	34.902
	Ω_4	111.037	103.313	94.546	85.477	78.001	74.266	57.694
	Ω_5	165.915	154.337	141.262	127.640	116.503	110.935	86.210
	Ω_1	8.566	7.970	7.294	6.594	6.017	5.729	4.451
	Ω_2	27.760	25.828	23.637	21.369	19.500	18.567	14.424
S-C	Ω_3	57.918	53.889	49.316	44.584	40.685	38.738	30.094
	Ω_4	99.043	92.153	84.333	76.242	69.574	66.244	51.462
	Ω_5	151.137	140.632	128.692	116.343	106.174	101.085	78.536
	Ω_1	8.566	7.970	7.294	6.594	6.017	5.729	4.451
	Ω_2	27.760	25.828	23.637	21.369	19.500	18.567	14.424
S-F	Ω_3	57.918	53.889	49.316	44.584	40.685	38.738	30.094
	Ω_4	99.043	92.153	84.333	76.241	69.573	66.244	51.462
	Ω_5	151.124	140.628	128.681	116.350	106.171	101.079	78.526
	Ω_1	12.430	11.566	10.584	9.569	8.732	8.314	6.459
	Ω_2	34.264	31.881	29.175	26.376	24.069	22.917	17.803
F-F	Ω_3	67.172	62.499	57.195	51.707	47.185	44.927	34.902
	Ω_4	111.039	103.314	94.547	85.475	77.998	74.267	57.695
	Ω_5	165.921	154.375	141.272	127.755	116.557	110.945	86.200

*Simsek [5].

considered in designing a beam to meet the required frequency. Changing this parameter also means changing flexibility of beams.

5.2. FG Beams with Elastically End Constraints

Three types of boundary condition; namely, C-E, S-E and E-E, of FG beams with elastically end constraints will be investigated in the following sections. Due to classical beam theory considered in this study, it is appropriate to choose the thickness ratio (L/h) more than 20. In the following investigation the ratio (L/h = 30) is selected for all of the next calculation. However, the frequency equation and mode shape function presented in this study can be used effectively for other values of the thickness ratio.

5.2.1. Vibration Analysis of FG Beams with C-E Boundary Condition

Consider a FG beam completely clamped at the left end and supported by translational and rotational springs at the right end. The beam is defined as the C-E beam. The frequency results for the first six modes with various volume fraction indexes are shown in **Table 4**. To verify the results, only the available work of Lai *et al*. [14] on the isotropic beam (n = 0 for full Al_2O_3) with the same type of support is shown in the second row. All modes of frequencies agree excellently. Again, all frequencies decrease as volume fraction indexes increase.

Effects of varying the values of spring constants, with n fixed at 0.5, on the response of FG beams for the first three modes are shown in **Table 5**. All frequencies increase as spring constants increase as expected. Observe

Table 4. Dimensionless frequencies of Al_2O_3/Al beams (L/h = 30, k_{TR} = 1.173 MN/m and k_{RR} = 1.056 × 10^3 MN·m/rad).

	Ω_1	Ω_2	Ω_3	Ω_4	Ω_5	Ω_6
n = 0	2.566	13.213	35.270	68.193	112.077	166.941
Lai *et al*. [14]	2.566	13.213	35.270	68.193	112.078	166.923
n = 0.2	2.547	12.970	34.493	66.611	109.420	162.902
n = 0.5	2.429	12.056	31.780	61.192	100.378	149.361
n = 1.0	2.305	11.112	28.987	55.605	91.051	135.293
n = 2.0	2.206	10.343	26.707	51.033	83.400	123.834
n = 5.0	2.171	9.987	25.611	48.803	79.643	118.170
n = 10.0	2.146	9.768	24.957	47.482	77.423	114.786

Table 5. Dimensionless frequencies of Al_2O_3/Al beams (n = 0.5; L/h = 30).

(MN/m)		k_{RR} (MN·m/rad)						
		1	10	10^2	10^3	10^4	10^5	10^6
k_{TR} = 1	Ω_1	2.051	2.056	2.102	2.383	2.788	2.891	2.903
	Ω_2	10.983	10.995	11.113	12.006	14.116	14.898	14.997
	Ω_3	30.617	30.628	30.745	31.726	35.036	36.755	36.994
k_{TR} = 10	Ω_1	3.669	3.670	3.678	3.733	3.826	3.853	3.856
	Ω_2	11.493	11.505	11.613	12.430	14.362	15.085	15.177
	Ω_3	30.793	30.805	30.920	31.890	35.144	36.831	37.067
k_{TR} = 10^2	Ω_1	6.737	6.739	6.766	6.969	7.492	7.710	7.738
	Ω_2	16.370	16.372	16.391	16.541	16.967	17.163	17.189
	Ω_3	32.806	32.816	32.911	33.704	36.300	37.649	37.839
k_{TR} = 10^3	Ω_1	7.553	7.559	7.616	8.091	9.669	10.544	10.673
	Ω_2	23.677	23.680	23.718	24.051	25.559	26.793	27.008
	Ω_3	46.330	46.331	46.336	46.385	46.612	46.809	46.844
k_{TR} = 10^4	Ω_1	7.637	7.644	7.705	8.213	9.932	10.897	11.038
	Ω_2	24.674	24.680	24.736	25.248	27.718	29.845	30.217
	Ω_3	51.235	51.240	51.293	51.786	54.615	57.896	58.574
k_{TR} = 10^5	Ω_1	7.646	7.652	7.713	8.225	9.958	10.932	11.074
	Ω_2	24.768	24.774	24.832	25.362	27.924	30.124	30.507
	Ω_3	51.653	51.659	51.717	52.262	55.410	59.017	59.746
k_{TR} = 10^6	Ω_1	7.647	7.653	7.714	8.226	9.961	10.935	11.078
	Ω_2	24.778	24.783	24.842	25.374	27.945	30.152	30.535
	Ω_3	51.693	51.699	51.758	52.309	55.486	59.122	59.855

that for very large value of k_{TR} and k_{RR}, the frequencies, Ω_1, Ω_2 and Ω_3 approach those of C-C beam in **Table 3**.

The first to forth mode shapes of FG beams with C-E boundary condition are shown in **Figures 5(a)-(d)**, respectively. It is seen that different values of spring support change the mode shapes of the vibrating beams significantly. Note that for $k_{TR} = k_{RR} = 0$, the beam corresponds to a C-F beam and as $k_{TR} = k_{RR} \to \infty$, a C-C beam is obtained.

5.2.2. Vibration Analysis of FG Beams with S-E Boundary Condition

Dimensionless frequency results of FG beams, with S-E boundary conditions as shown in **Figure 4**, for the first six modes are tabulated in **Table 6**. To verify the results, again, only the work of Lai *et al*. [14] on the isotropic beam ($n = 0$) is available as shown in the second row of **Table 6**. All frequencies, Ω_1 to Ω_6, agree excellently. It is seen that, all frequencies decrease as volume fraction indexes increase.

The first three frequencies for S-E boundary condition with variable spring constants, k_{TR} and k_{RR} are presented in **Table 7**. To illustrate the effects of spring constants and material volume fraction on the fundamental frequency, 3-D figures for S-E and C-E beams are plotted in **Figure 6**. And **Figure 7** shows the 1st to 4th mode shapes of FG beams with S-E boundary condition.

5.2.3. Vibration Analysis of FG Beams with E-E Boundary Condition

FG beams supported by translational and rotational springs at both ends as shown in **Figure 2** are considered in this section. Dimensionless frequencies of various modes and volume fraction indexes are presented in **Table 8**. Again, the accuracy is confirmed by the case of isotropic beams by Lai *et al*. [14]. It is observed that the first and second frequency results depend mostly on the effects of translational and rotational spring stiffnesses at both ends, Hence, they show different trends of change in comparison with other modes when the value of the

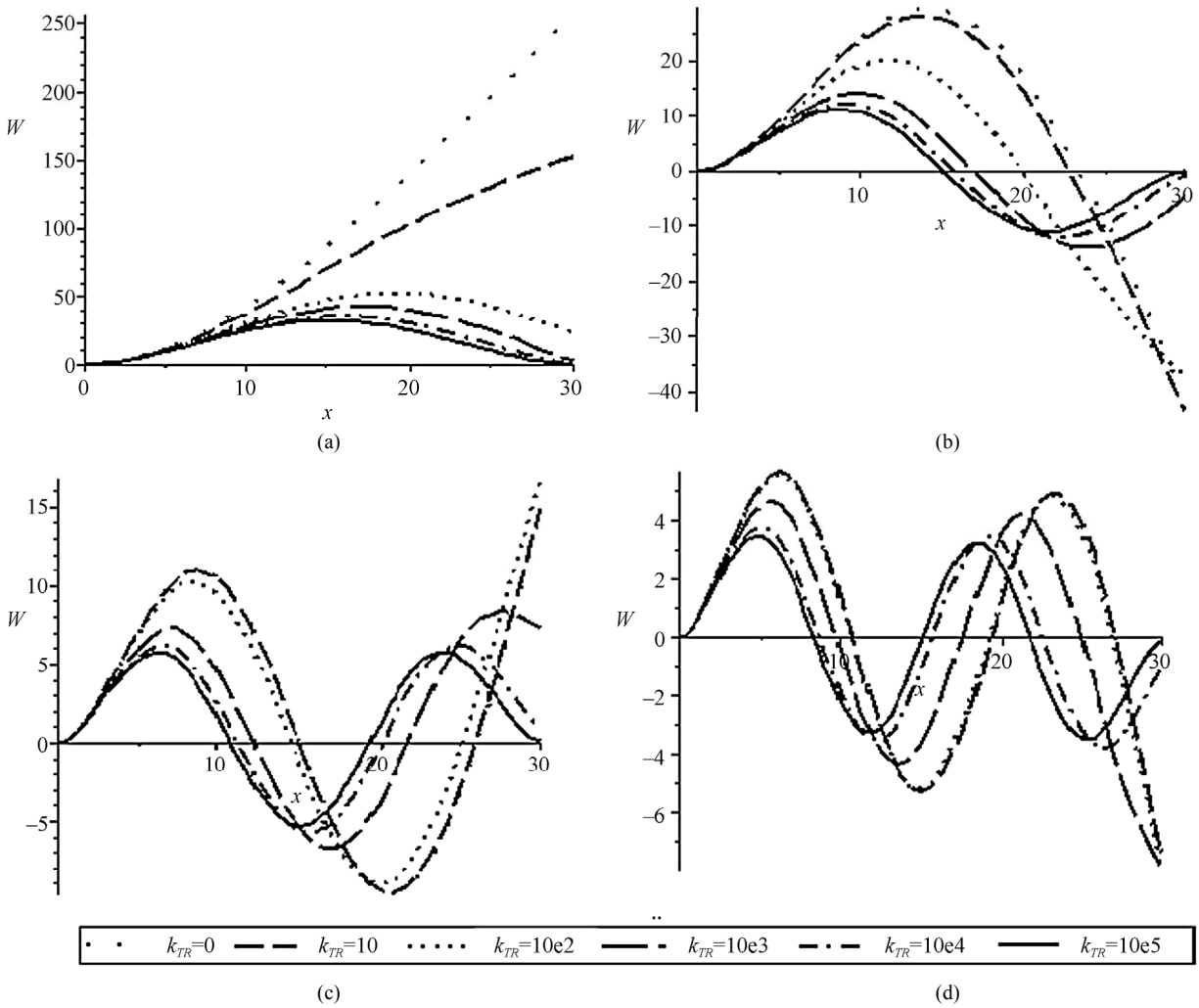

Figure 5. The 1st to 4th mode shapes of Al_2O_3/Al beams with C-E boundary conditions ($n = 0.5$; $L/h = 30$; $k_{TR} = k_{RR}$).

Table 6. Dimensionless frequency results of Al_2O_3/Al beams (L/h = 30; k_{TR} = 29.32 MN/m; k_{RR} = 0 MN·m/rad).

	Ω_1	Ω_2	Ω_3	Ω_4	Ω_5	Ω_6
n = 0	3.826	10.471	28.340	58.189	99.200	151.238
Lai *et al*. [14]	3.826	10.471	28.340	58.189	99.200	151.238
n = 0.2	3.843	10.412	27.707	56.785	96.773	147.525
n = 0.5	3.736	10.001	25.517	52.039	88.603	135.026
n = 1.0	3.576	9.616	23.284	47.142	80.156	122.113
n = 2.0	3.411	9.355	21.493	43.128	73.207	111.470
n = 5.0	3.331	9.322	20.663	41.150	69.752	106.164
n = 10.0	3.273	9.282	20.176	39.986	67.718	103.042

Table 7. Dimensionless frequencies of Al_2O_3/Al beams (n = 0.5; L/h = 30).

(MN/m)		k_{RR} (MN·m/rad)						
		1	10	10^2	10^3	10^4	10^5	10^6
k_{TR} = 1	Ω_1	0.929	0.933	0.968	1.160	1.386	1.437	1.442
	Ω_2	7.725	7.736	7.849	8.662	10.379	10.959	11.031
	Ω_3	24.803	24.815	24.931	25.893	28.919	30.378	30.577
k_{TR} = 10	Ω_1	2.652	2.652	2.652	2.653	2.654	2.655	2.655
	Ω_2	8.455	8.464	8.558	9.239	10.707	11.216	11.279
	Ω_3	25.022	25.034	25.148	26.093	29.048	30.471	30.665
k_{TR} = 10^2	Ω_1	4.503	4.507	4.544	4.830	5.549	5.845	5.884
	Ω_2	13.800	13.800	13.803	13.830	13.906	13.940	13.945
	Ω_3	27.559	27.567	27.650	28.331	30.434	31.470	31.613
k_{TR} = 10^3	Ω_1	4.855	4.860	4.916	5.362	6.689	7.345	7.437
	Ω_2	18.907	18.911	18.955	19.339	21.004	22.274	22.488
	Ω_3	40.260	40.261	40.274	40.392	40.944	41.430	41.519
k_{TR} = 10^4	Ω_1	4.891	4.897	4.954	5.418	6.818	7.517	7.615
	Ω_2	19.513	19.519	19.576	20.088	22.404	24.226	24.532
	Ω_3	43.716	43.722	43.776	44.278	47.059	50.075	50.673
k_{TR} = 10^5	Ω_1	4.895	4.901	4.958	5.424	6.831	7.534	7.633
	Ω_2	19.572	19.578	19.636	20.161	22.540	24.408	24.720
	Ω_3	44.018	44.023	44.082	44.625	47.648	50.896	51.530
k_{TR} = 10^6	Ω_1	4.895	4.901	4.959	5.425	6.832	7.535	7.634
	Ω_2	19.578	19.584	19.642	20.168	22.553	24.426	24.739
	Ω_3	44.047	44.053	44.112	44.659	47.706	50.975	51.611

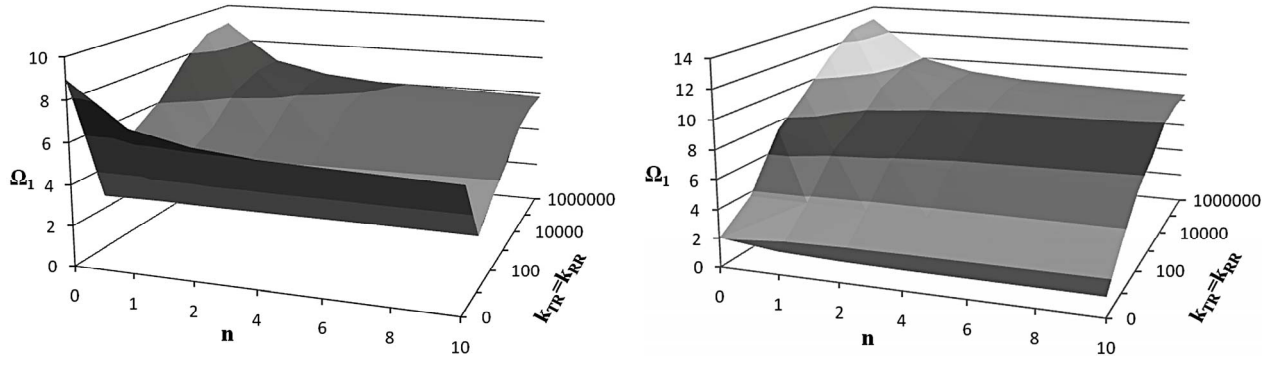

(a) S-E (b) C-E

Figure 6. Fundamental frequency of Al_2O_3/Al beams with S-E and C-E boundary conditions (L/h = 30).

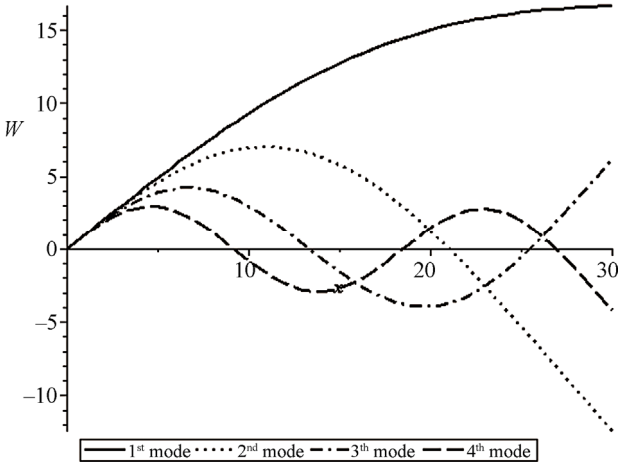

Figure 7. The 1st to 4th mode shapes of Al_2O_3/Al beams with S-E boundary conditions (n = 0.5; L/h = 30; k_{TR} = 10 MN/m, k_{RR} = 10 MN·m/rad).

volume fraction index increases. It is clear that as the values of $k_{TL} = k_{TR} = k_{RL} = k_{RR} \to \infty$, this E-E FG beam behaves like the C-C FG beam (see **Table 3**).

Table 9 shows the frequency results of the first three modes with variable spring constants. It is similar to the previous cases that frequencies increase as the spring constants increase.

To understand the vibration behavior of FG beams supported by elastically end constraints, the effect of spring constants at both ends on the fundamental frequencies is shown as 3-D plot in **Figure 8**. **Figure 9** shows the 1st to 4th mode shapes of E-E beams. It is observed that the first mode shape depends mostly on the translational springs which move up and down, including a small bending along the length of the beam. But for the second mode shape, it seems to be dependent on the rotational springs in which the movement is clockwise and

Table 8. Dimensionless frequencies of Al_2O_3/Al beams (L/h = 30; $k_{TL} = k_{TR}$ = 1.173 MN/m; $k_{RL} = k_{RR} = 1.056 \times 10^3$ MN·m/rad).

	Ω_1	Ω_2	Ω_3	Ω_4	Ω_5	Ω_6
n = 0	0.781	2.771	14.243	36.242	69.209	113.112
Lai *et al*. [14]	0.781	2.771	14.242	-	-	-
n = 0.2	0.802	2.822	14.046	35.532	67.700	110.531
n = 0.5	0.825	2.838	13.206	32.943	62.419	101.637
n = 1.0	0.849	2.838	12.343	30.290	56.994	92.486
n = 2.0	0.876	2.833	11.653	28.148	52.588	85.025
n = 5.0	0.906	2.858	11.364	27.163	50.494	81.420
n = 10.0	0.920	2.861	11.178	26.566	49.245	79.284

Table 9. Dimensionless frequencies of Al_2O_3/Al beams (n = 0.5; L/h = 30).

(MN/m) $k_{TL} = k_{TR}$		$k_{RL} = k_{RR}$ (MN·m/rad)						
		1	10	10^2	10^3	10^4	10^5	10^6
1	Ω_1	0.760	0.760	0.760	0.762	0.765	0.766	0.766
	Ω_2	1.330	1.355	1.582	2.746	4.439	4.945	5.006
	Ω_3	11.204	11.226	11.444	13.112	17.442	19.325	19.579
10	Ω_1	2.208	2.209	2.218	2.275	2.361	2.384	2.386
	Ω_2	4.144	4.150	4.212	4.658	5.596	5.924	5.966
	Ω_3	12.144	12.163	12.355	13.842	17.836	19.611	19.852
10^2	Ω_1	4.213	4.221	4.293	4.823	6.031	6.487	6.545
	Ω_2	11.536	11.536	11.536	11.538	11.543	11.546	11.546
	Ω_3	19.378	19.384	19.445	19.952	21.611	22.494	22.621
10^3	Ω_1	4.816	4.828	4.937	5.811	8.529	10.070	10.305
	Ω_2	18.314	18.323	18.406	19.133	22.115	24.313	24.683
	Ω_3	37.532	37.535	37.565	37.832	39.012	39.962	40.127
10^4	Ω_1	4.888	4.899	5.014	5.936	8.922	10.705	10.983
	Ω_2	19.450	19.461	19.575	20.585	25.188	29.146	29.864
	Ω_3	43.392	43.403	43.509	44.497	49.920	56.023	57.300
10^5	Ω_1	4.895	4.907	5.022	5.949	8.963	10.772	11.054
	Ω_2	19.566	19.578	19.695	20.736	25.521	29.675	30.430
	Ω_3	43.986	43.997	44.114	45.196	51.223	58.101	59.537
10^6	Ω_1	4.896	4.907	5.023	5.951	8.967	10.779	11.061
	Ω_2	19.578	19.589	19.707	20.751	25.555	29.728	30.486
	Ω_3	44.044	44.056	44.174	45.265	51.352	58.304	59.754

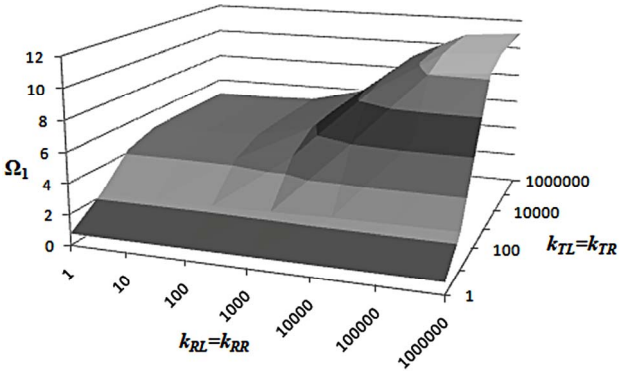

Figure 8. The fundamental frequency of Al_2O_3/Al beams with E-E boundary condition (n = 0.5; L/h = 30).

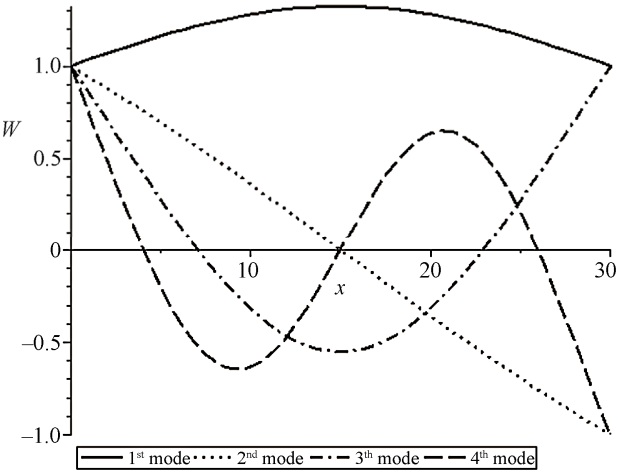

Figure 9. The 1st to 4th mode shape of Al_2O_3/Al beams with E-E boundary conditions (n = 0.5; L/h = 30; k_{TR} = 10 MN/m; k_{RR} = 10 MN·m/rad).

anti-clockwise. If the spring constant becomes large, the mode shapes of E-E beams behave like C-C beams.

6. Concluding Remarks

This research applies the differential transformation method to solve the governing differential equation of free vibration of functionally graded beams supported by various types of general boundary conditions, including elastically end constraints. FG beams made of Al_2O_3/Al are chosen to study the free vibration behavior. In general, the results revealed that trend of frequency results for various modes of vibration decreases as the volume fraction indexes increase, except for the case of the E-E boundary conditions in which the trend of the first two modes is reversed owning to the effects of translational and rotational springs at both ends. It is also seen that there are considerable changes of frequencies as well as mode shapes when the stiffness of spring becomes larger. The frequency equation and mode function presented in this study can be specialized to approximate any other boundary conditions, with or without springs, by setting the values of spring constants as appropriate.

REFERENCES

[1] B. V. Sankar, "An Elasticity Solution for Functionally Graded Beams," *Composites Science and Technology*, Vol. 61, No. 5, 2001, pp. 689-696. doi:10.1016/S0266-3538(01)00007-0

[2] Z. Zhong and T. Yu, "Analytical Solution of a Cantilever Functionally Graded Beam," *Composites Science and Technology*, Vol. 67, No. 3-4, 2007, pp. 481-488. doi:10.1016/j.compscitech.2006.08.023

[3] S. Kapuria, M. Bhattacharyya and A. N. Kumar, "Bending and Free Vibration Response of Layered Functionally Graded Beams: A Theoretical Model and Its Experimental Validation," *Composite Structures*, Vol. 82, No. 3, 2008, pp. 390-402. doi:10.1016/j.compstruct.2007.01.019

[4] S. A. Sina, H. M. Navazi and H. Haddadpour, "An Analytical Method for Free Vibration Analysis of Functionally Graded Beams," *Materials & Design*, Vol. 30, No. 3, 2009, pp. 741-747. doi:10.1016/j.matdes.2008.05.015

[5] M. Simsek, "Fundamental Frequency Analysis of Functionally Graded Beams by Using Different Higher-Order Beam Theories," *Nuclear Engineering and Design*, Vol. 240, No. 4, 2010, pp. 697-705. doi:10.1016/j.nucengdes.2009.12.013

[6] M. Aydogdu and V. Taskin, "Free Vibration Analysis of Functionally Graded Beams with Simply Supported Edges," *Materials & Design*, Vol. 28, No. 5, 2007, pp. 1651-1656. doi:10.1016/j.matdes.2006.02.007

[7] N. Wattanasakulpong, B. G. Prusty, D. W. Kelly and M. Hoffman, "A Theoretical Investigation on the Free Vibration of Functionally Graded Beams," *Proceedings of the 10th International Conference on Computational Structures Technology*, Valencia, 14-17 September 2010, p. 285.

[8] E. Alshorbagy Amal, M. A. Eltaher and F. F. Mahmoud, "Free Vibration Characteristics of a Functionally Graded Beam by Finite Element Method," *Applied Mathematical Modelling*, Vol. 35, No. 1, 2011, pp. 412-425. doi:10.1016/j.apm.2010.07.006

[9] J. Yang and Y. Chen, "Free Vibration and Buckling Analysis of Functionally Graded Beams with Edge Cracks," *Composite Structures*, Vol. 83, No. 1, 2008, pp. 48-60. doi:10.1016/j.compstruct.2007.03.006

[10] S. Kitipornchai, L. L. Ke, J. Yang and Y. Xiang, "Nonlinear Vibration of Edge Cracked Functionally Graded Timoshenko Beams," *Journal of Sound and Vibration*, Vol. 324, No. 3-5, 2009, pp. 962-982. doi:10.1016/j.jsv.2009.02.023

[11] S. Sahraee and A. R. Saidi, "Free Vibration and Buckling Analysis of Functionally Graded Deep Beam-Columns on Two-Parameter Elastic Foundations Using the Differential Quadrature Method," *Journal of Mechanical Engineering Sci*ence, Vol. 223, No. 6, 2009, pp. 1273-1284. doi:10.1243/09544062JMES1349

[12] S. C. Pradhan and T. Murmu, "Thermo-Mechanical Vi-

bration of FGM Sandwich Beam under Variable Elastic Foundations Using Differential Quadrature Method," *Journal of Sound and Vibration*, Vol. 321, No. 1-2, 2009, pp. 342-362. doi:10.1016/j.jsv.2008.09.018

[13] J. C. Hsu, H. Y. Lai and C. K. Chen, "Free Vibration of Non-Uniform Euler-Bernoulli Beams with General Elastically End Constraints Using Adomain Modified Decomposition Method," *Journal of Sound and Vibration*, Vol. 318, No. 4-5, 2008, pp. 965-981.

[14] H. Y. Lai, J. C. Hsu and C. K. Chen, "An Innovative Eigenvalue Problem Solver for Free Vibration of Euler-Bernoulli Beam by Using the Adomain Decomposition Method," *Computers & Mathematics with Applications*, Vol. 56, No. 12, 2008, pp. 3204-3220. doi:10.1016/j.camwa.2008.07.029

[15] Y. Liu and C. S. Gurram, "The Use of He's Variational Iteration Method for Obtaining the Free Vibration of an Euler-Bernoulli Beam," *Mathematical and Computer Modelling*, Vol. 50, No. 11-12, 2009, pp. 1545-1552. doi:10.1016/j.mcm.2009.09.005

[16] Q. Mao and S. Pietrzko, "Free Vibration Analysis of Stepped Beams by Using Adomian Decomposition Method," *Applied Mathematics and Computation*, Vol. 217, No. 7, 2010, pp. 3429-3441. doi:10.1016/j.amc.2010.09.010

[17] J. K. Zhou, "Differential Transformation and Its Application for Electrical Circuits," Huazhong University Press, Wuhan, 1986.

[18] M. Malik and H. H. Dang, "Vibration Analysis of Continuous Systems by Differential Transformation," *Applied Mathematics and Computation*, Vol. 96, No. 1, 1998, pp. 17-26. doi:10.1016/S0096-3003(97)10076-5

[19] M. O. Kaya and O. O. Ozgumus, "Flexural-Torsional-Coupled Vibration Analysis of Axially Loaded Closed-Section Composite Timoshenko Beam by Using DTM," *Journal of Sound and Vibration*, Vol. 306, No. 3-5, 2007, pp. 495-506.

[20] O. O. Ozgumus and M. O. Kaya, "Flapwise Bending Vibration Analysis of Double Tapered Rotating Euler-Burnoulli Beam by Using the Differential Transform Method," *Meccanica*, Vol. 41, No. 6, 2006, pp. 661-670. doi:10.1007/s11012-006-9012-z

[21] O. O. Ozgumus and M. O. Kaya, "Vibration Analysis of a Rotating Tapered Timoshenko Beam Using DTM," *Meccanica*, Vol. 45, No. 1, 2010, pp. 33-42. doi:10.1007/s11012-009-9221-3

[22] S. C. Pradhan and G. K. Reddy, "Buckling Analysis of Single Walled Carbon Nanotube on Winkler Foundation Using Nonlocal Elasticity Theory and DTM," *Computational Materials Science*, Vol. 50, No. 3, 2011, pp. 1052-1056. doi:10.1016/j.commatsci.2010.11.001

[23] F. Delale and F. Erdogan, "The Crack Problem for a Non-Homogeneous Plane," *Journal of Applied Mechanics*, Vol. 50, No. 3, 1983, pp. 609-614. doi:10.1115/1.3167098

Appendix A

S-S

The frequency equation:

$$\sum_{r=0}^{R}\frac{\omega^{2r}I_0^rL^{(4r+1)}}{\lambda^r(4r+1)!}\times\sum_{r=0}^{R}\frac{\omega^{2r}I_0^rL^{(4r+1)}}{\lambda^r(4r+1)!}-\sum_{r=1}^{R}\frac{\omega^{2r}I_0^rL^{(4r-1)}}{\lambda^r(4r-1)!}\times\sum_{r=0}^{R}\frac{\omega^{2r}I_0^rL^{(4r+3)}}{\lambda^r(4r+3)!}=0$$

The mode shape function:

$$W(x)=\sum_{r=0}^{R}\frac{\omega^{2r}I_0^r}{\lambda^r(4r+1)!}x^{(4r+1)}-\frac{\sum_{r=0}^{R}\frac{\omega^{2r}I_0^rL^{(4r+1)}}{\lambda^r(4r+1)!}}{\sum_{r=0}^{R}\frac{\omega^{2r}I_0^rL^{(4r+3)}}{\lambda^r(4r+3)!}}\sum_{r=0}^{R}\frac{\omega^{2r}I_0^r}{\lambda^r(4r+3)!}x^{(4r+3)}$$

S-C

The frequency equation:

$$\sum_{r=0}^{R}\frac{\omega^{2r}I_0^rL^{(4r+1)}}{\lambda^r(4r+1)!}\times\sum_{r=0}^{R}\frac{\omega^{2r}I_0^rL^{(4r+2)}}{\lambda^r(4r+2)!}-\sum_{r=0}^{R}\frac{\omega^{2r}I_0^rL^{(4r)}}{\lambda^r(4r)!}\times\sum_{r=0}^{R}\frac{\omega^{2r}I_0^rL^{(4r+3)}}{\lambda^r(4r+3)!}=0$$

The mode shape function:

$$W(x)=\sum_{r=0}^{R}\frac{\omega^{2r}I_0^r}{\lambda^r(4r+1)!}x^{(4r+1)}-\frac{\sum_{r=0}^{R}\frac{\omega^{2r}I_0^rL^{(4r+1)}}{\lambda^r(4r+1)!}}{\sum_{r=0}^{R}\frac{\omega^{2r}I_0^rL^{(4r+3)}}{\lambda^r(4r+3)!}}\sum_{r=0}^{R}\frac{\omega^{2r}I_0^r}{\lambda^r(4r+3)!}x^{(4r+3)}$$

S-F

The frequency equation:

$$\sum_{r=1}^{R}\frac{\omega^{2r}I_0^rL^{(4r-1)}}{\lambda^r(4r-1)!}\times\sum_{r=0}^{R}\frac{\omega^{2r}I_0^rL^{(4r)}}{\lambda^r(4r)!}-\sum_{r=1}^{R}\frac{\omega^{2r}I_0^rL^{(4r-2)}}{\lambda^r(4r-2)!}\times\sum_{r=0}^{R}\frac{\omega^{2r}I_0^rL^{(4r+1)}}{\lambda^r(4r+1)!}=0$$

The mode shape function:

$$W(x)=\sum_{r=0}^{R}\frac{\omega^{2r}I_0^r}{\lambda^r(4r+1)!}x^{(4r+1)}-\frac{\sum_{r=1}^{R}\frac{\omega^{2r}I_0^rL^{(4r-1)}}{\lambda^r(4r-1)!}}{\sum_{r=0}^{R}\frac{\omega^{2r}I_0^rL^{(4r+1)}}{\lambda^r(4r+1)!}}\sum_{r=0}^{R}\frac{\omega^{2r}I_0^r}{\lambda^r(4r+3)!}x^{(4r+3)}$$

C-F

The frequency equation:

$$\sum_{r=0}^{R}\frac{\omega^{2r}I_0^rL^{(4r)}}{\lambda^r(4r)!}\times\sum_{r=0}^{R}\frac{\omega^{2r}I_0^rL^{(4r)}}{\lambda^r(4r)!}-\sum_{r=1}^{R}\frac{\omega^{2r}I_0^rL^{(4r-1)}}{\lambda^r(4r-1)!}\times\sum_{r=0}^{R}\frac{\omega^{2r}I_0^rL^{(4r+1)}}{\lambda^r(4r+1)!}=0$$

The mode shape function:

$$W(x)=\sum_{r=0}^{R}\frac{\omega^{2r}I_0^r}{\lambda^r(4r+2)!}x^{(4r+2)}-\frac{\sum_{r=0}^{R}\frac{\omega^{2r}I_0^rL^{(4r)}}{\lambda^r(4r)!}}{\sum_{r=0}^{R}\frac{\omega^{2r}I_0^rL^{(4r+1)}}{\lambda^r(4r+1)!}}\sum_{r=0}^{R}\frac{\omega^{2r}I_0^r}{\lambda^r(4r+3)!}x^{(4r+3)}$$

C-C

The frequency equation:

$$\sum_{r=0}^{R}\frac{\omega^{2r}I_0^rL^{(4r+2)}}{\lambda^r(4r+2)!}\times\sum_{r=0}^{R}\frac{\omega^{2r}I_0^rL^{(4r+2)}}{\lambda^r(4r+2)!}-\sum_{r=0}^{R}\frac{\omega^{2r}I_0^rL^{(4r+1)}}{\lambda^r(4r+1)!}\times\sum_{r=0}^{R}\frac{\omega^{2r}I_0^rL^{(4r+3)}}{\lambda^r(4r+3)!}=0$$

The mode shape function:

$$W(x)=\sum_{r=0}^{R}\frac{\omega^{2r}I_0^r}{\lambda^r(4r+2)!}x^{(4r+2)}-\frac{\sum_{r=0}^{R}\frac{\omega^{2r}I_0^rL^{(4r+2)}}{\lambda^r(4r+2)!}}{\sum_{r=0}^{R}\frac{\omega^{2r}I_0^rL^{(4r+3)}}{\lambda^r(4r+3)!}}\sum_{r=0}^{R}\frac{\omega^{2r}I_0^r}{\lambda^r(4r+3)!}x^{(4r+3)}$$

